Zeeman frequency shifts in an optical dipole trap used to search for an electric-dipole moment

M. V. Romalis and E. N. Fortson
Department of Physics, University of Washington, Seattle, Washington 98195
(Received 12 October 1998)

We calculate the Zeeman frequency shifts due to interactions with the light in a far-off-resonance optical dipole trap. These shifts are important for potential use of such a trap to search for an atomic permanent electric-dipole moment (EDM). We present numerical results for Cs and Hg, as examples of paramagnetic and diamagnetic atoms. The vector and tensor light shifts are calculated for a large range of trap optical frequencies, for both red-detuned and blue-detuned traps. We also consider frequency shifts resulting from magnetic dipole and electric quadrupole transitions mixed in by a static electric field. These shifts are particularly important for EDM experiments since they are linear in the electric field. The Zeeman frequency shifts represent a substantial problem for EDM experiments in a dipole trap and must be controlled with care to achieve theoretical sensitivity. [S1050-2947(99)02806-1]

PACS number(s): 32.80.Pj, 32.60.+i, 32.10.Dk, 11.30.Er

I. INTRODUCTION

The search for a permanent electric-dipole moment (EDM) is an effective method of probing for physics beyond the standard model [1]. A nonzero value of the EDM requires violation of T and P invariance. If the CPT symmetry is not violated, it also implies CP violation. Within the standard model the EDMs are unmeasurably small, but many extensions of the standard model predict EDMs well within experimental reach. Techniques of laser cooling and trapping of neutral atoms open new possibilities for EDM experiments [2,3]. In one of the more promising methods, cold atoms are held between high-voltage electrodes in an optical dipole trap, and the coupling between the static electric field and the atomic EDM produces a shift of the Zeeman levels of the atoms. However, the Zeeman levels would also be shifted by the interactions with the trapping laser fields. In this paper we present a systematic analysis of the various Zeeman energy shifts due to the laser fields in an optical dipole trap, and discuss how they might limit the sensitivity of an EDM experiment. We find that such shifts will impose tight constraints on the design of the experiment.

An atom with a permanent electric-dipole moment d and a magnetic dipole moment μ interacts with electric and magnetic fields $\boldsymbol{E}$ and $\boldsymbol{B}$ according to the following Hamiltonian,

$$H = -(d\boldsymbol{E} + \mu\boldsymbol{B}) \cdot \frac{\boldsymbol{F}}{F}, \tag{1}$$

where $\boldsymbol{F}$ is the total atomic angular momentum. To detect an EDM the Zeeman precession frequency is measured in parallel electric and magnetic fields. A change of the Zeeman frequency correlated with the reversal of $\boldsymbol{E}$ relative to $\boldsymbol{B}$ would indicate the presence of a permanent EDM. A frequency measurement performed on a classical ensemble of N atoms with Zeeman coherence time τ has a shot-noise limited uncertainty $\delta\omega = \tau^{-1}N^{-1/2}$. If the measurement is done repeatedly for a time $T \gg \tau$, the resulting uncertainty in EDM is given by

$$\delta d = \frac{\hbar}{2E\sqrt{\tau N T}}, \tag{2}$$

omitting a factor of order unity, which depends on the specific experimental arrangement. EDM measurements so far have been performed in an atomic beam [4] or in a cell [5–8]. Each type of experiment has its advantages and limitations. Beam experiments allow application of a larger electric field, while cell experiments have the advantage of longer coherence times. In beam experiments the systematic errors due to $\boldsymbol{v}\times\boldsymbol{E}$ magnetic fields often limit achievable sensitivity, while in cell experiments the leakage currents can produce systematic errors, which are difficult to estimate.

Using cold atoms it may be possible to combine the advantages of beam and cell experiments, having both long coherence times and large E fields, while eliminating the systematic errors due to both the $\boldsymbol{v}\times\boldsymbol{E}$ fields and the leakage currents. EDM measurements with laser-cooled atoms in a trap or a fountain have been proposed [2,3]. In this paper we concentrate on neutral atom traps. Since EDM experiments rely on a measurement of the Zeeman precession frequency, the atom trap cannot rely on inhomogeneous magnetic fields. Among various neutral atom traps the most promising appears to be an optical dipole trap [3,9]. In this trap the polarizability of the atoms provides the trapping force in a light beam. If the frequency of the light is tuned below (above) the resonance frequency of the atoms, they are attracted to the maximum (minimum) of the light intensity. The optical dipole trap creates a conservative force, i.e., it does not cool the atoms. They are heated due to scattering of photons from the trapping beam. However, the heating rate can be reduced by detuning the frequency of the trapping laser very far from the atomic resonances [10–12]. The spin relaxation due to light scattering can also be made negligible [12].

In this paper we consider the effects of the trapping beam and the static electric field, which result in frequency shifts of the Zeeman transitions. These shifts can be divided into three classes. Residual circular polarization of the trapping beam produces a vector light shift of the Zeeman levels [13]. This shift is linear in m, the projection of the total angular

momentum $\boldsymbol{F}$ onto the quantization axis. Hyperfine interactions in the excited state cause tensor shifts due to the trapping light [13] and the static electric field [14,15], which are quadratic in m. Finally, in the presence of the static electric field the atomic levels acquire a small admixture of opposite parity states, allowing an interference of the electric-dipole amplitude with the magnetic dipole and electric quadrupole amplitudes [16,17]; the resulting shifts of the Zeeman levels are proportional to the electric field, and, to that extent, have the same signature as an EDM.

Most of the calculations are performed for a single trapping beam, detuned to the red of all atomic resonance lines. A separate section is devoted to the calculation of the average Zeeman shifts in a blue-detuned trap, which is particularly suitable for EDM experiments in paramagnetic atoms. We consider the trapping beam frequencies from dc up to within tens of GHz of the atomic resonance lines. Thus, we include the counter-rotating components of the oscillating fields and the contribution of the hyperfine mixing between different excited states. We assume that the detuning of the trapping beam is much larger than the excited state hyperfine structure, which is treated as a perturbation. The vector and tensor light shifts of the Zeeman levels have been calculated previously near the resonance [13]. The tensor light shift due to a static electric field has been calculated in [14,15]. Hyperfine light shifts for Cs in an optical dipole trap have been studied in [3]. To our knowledge, the Zeeman frequency shifts due to multipole interference in an electric field have not been calculated before.

The searches for an EDM are usually done in heavy atoms, since the sensitivity to T-violating interactions increases rapidly with Z. Atoms with and without unbalanced electron spin (paramagnetic and diamagnetic) should be treated separately since they are sensitive to different types of fundamental T-violating interactions [1]. Paramagnetic atoms are sensitive to an electron EDM, while diamagnetic atoms with a nuclear spin are sensitive to hadronic sources of T violation. Both types of atoms are sensitive to semileptonic T-violating interactions. Among paramagnetic atoms, Cs is a prime candidate for initial experiments in a trap, because it is moderately heavy ($Z=55$), and laser cooling and trapping techniques for Cs are well developed. For future experiments Fr ($Z=87$) is also a possible candidate [18]. Its sensitivity to an electron EDM is a factor of 10 larger than Cs [19], but it has a half-life of only 20 min. Among paramagnetic atoms we choose Cs for our calculations.

Among diamagnetic atoms, Hg ($Z=80$) has been used so far to set the best limits on an atomic EDM originating from nuclear interactions [5]. However, laser cooling and trapping of Hg is difficult because its resonance lines are far in the UV (254 and 185 nm). Yb ($Z=70$) offers a good compromise for initial experiments. Its sensitivity to P,T-odd interactions is smaller by about a factor of 3 than Hg [20,21], but it is much easier to cool using resonance lines at 556 and 398 nm. Like Hg, it has an isotope with $I=1/2$, for which the tensor shifts of the Zeeman levels are absent. For future experiments Ra ($Z=88$) offers an interesting possibility. Recent calculations [22] show that due to close lying opposite parity nuclear states, the P,T-odd interactions in Ra are enhanced by a factor of 500 compared with Hg. We performed the calculations for Hg, since it has a relatively simple atomic structure, and the shifts for other diamagnetic atoms should have the same order of magnitude.

To ascertain the significance of the Zeeman frequency shifts calculated below, we estimate, using Eq. (2), the required frequency sensitivity necessary to be competitive with present limits on EDMs. We assume that the experiments can be performed with an electric field of 100 kV/cm. To be competitive with the present limit on the electron EDM set by the Tl experiment [4], the Zeeman frequency shift in Cs has to be measured with a precision of about 5 μHz. To be competitive with the present limit set on Hg EDM [5], the Zeeman frequency shift in Hg has to be measured with a precision of 10 nHz. In proposed experiments with Cs [2] and Yb [21] it has been assumed that one can trap $N=10^8$ atoms with a coherence time $\tau=10$ s. These numbers have already been achieved, although not in the same experiment [23,24]. They result in a shot-noise limited frequency uncertainty of 5 $\mu\mathrm{Hz}/\sqrt{\mathrm{Hz}}$. If one can achieve this sensitivity, then the Cs experiment can improve the limit on the electron EDM by a factor of 100 with an integration time on the order of one day.

For experiments with diamagnetic atoms, much longer integration times are required. However, fermionic atoms with $^1S_0$ ground state offer a number of advantages, which may allow one to substantially increase the number of trapped atoms and the coherence time. For two identical fermions in the same spin state the s-wave scattering cross section vanishes, while p and higher scattering cross sections go to zero at sufficiently low temperatures. Thus, in spin-polarized fermionic atoms most of the effects that might limit the density of atoms and the coherence time, such as elastic collisions, three-body recombination rates, collisional frequency shifts, and collisional spin relaxation, are greatly reduced. Spin-polarized fermionic atoms held in a conservative trap would give the closest approximation yet to an interaction-free sample of atoms. For atoms with $^1S_0$ ground state, such as Hg or Yb, these effects may also be suppressed compared to alkali atoms even in the absence of perfect spin polarization. Therefore, we believe that $N=10^9$ and $\tau=100$ sec are reasonable goals for fermionic species with $^1S_0$ ground state. This gives a shot-noise sensitivity of 500 $\mathrm{nHz}/\sqrt{\mathrm{Hz}}$. To improve the present limit on the Hg EDM by a factor of 100 would require an integration time of 300 days. This difference in the integration time required for paramagnetic and diamagnetic atoms already exists in the present experiments. The Tl EDM experiment [4] achieves its statistical precision in 6 days, while the Hg experiment [5] takes 300 days.

This paper is organized as follows. In Sec. II we introduce our notation and approximations. The photon scattering rate and the spin relaxation rate due to Raman scattering in a red-detuned trap are also calculated. Sec. III is devoted to the vector and tensor light shifts in a red-detuned trap, while in Sec. IV we calculate the vector and tensor shifts for Cs in a blue-detuned trap. In Sec. V we calculate the shifts due to the magnetic dipole and electric quadrupole transitions in the presence of a static electric field, and discuss how one can design an EDM experiment to minimize the size of the Zeeman shifts.

II. TRAPPING POTENTIAL AND PHOTON SCATTERING RATE

We begin by calculating the depth and the photon scattering rate for a far-off-resonance red-detuned dipole trap.

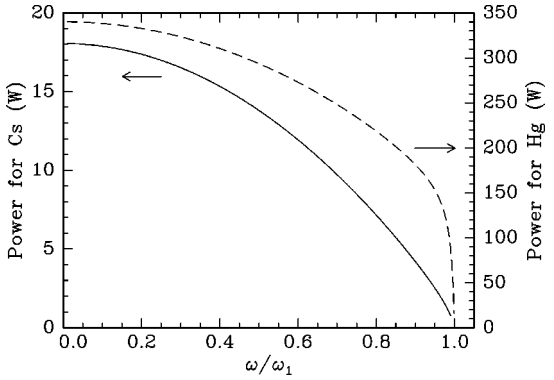

FIG. 1. Laser power required to achieve a trap depth of 100 μK with beam spot size of 100 μm. ω_1 is the lowest atomic resonance frequency, $6P_{1/2}$ for Cs (solid line plotted against the left axis) and 6^3P_1 for Hg (broken line plotted against the right axis).

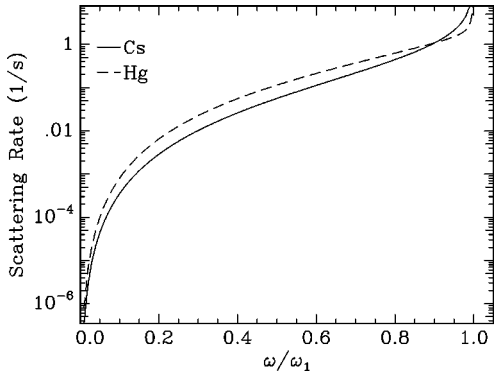

FIG. 2. Rayleigh scattering rate for Cs (solid line) and Hg (broken line) for linearly polarized light. ω_1 is the lowest resonance frequency of the atom.

Similar calculations have been done in Refs. [10,11]. We include these results here for completeness and to introduce the notation and the approximations used throughout the paper.

The electric field of the trapping beam near the center of the trap is given by

$$\boldsymbol{E}=\frac{E_0}{2}(\hat{\boldsymbol{\varepsilon}}e^{-i\omega t}+\hat{\boldsymbol{\varepsilon}}^*e^{i\omega t}). \tag{3}$$

For a Gaussian beam focused to a spot size w_0, the total power is $P=cE_0^2w_0^2/16$. In the regime when the population of the excited state is small, the depth of the trap is given by [25]

$$U=-\frac{e^2E_0^2}{4m}\left[\sum_e \frac{f_e}{\omega_e^2-\omega^2}+\int_{\omega_I}^{\infty}\frac{(df/d\omega')d\omega'}{(\omega'-\omega_e)^2-\omega^2}\right], \tag{4}$$

where $\hbar\omega_e$ is the energy of the excited states with respect to the ground state and f_e is the oscillator strength. The first term is a sum over the discrete excited states of the atom, while the second term gives the contribution of the continuum above the ionization energy. For ω much less than the lowest atomic resonance frequency ω_1 the depth of the trap is given by the static atomic polarizability α_s,

$$U=-\tfrac{1}{4}\alpha_sE_0^2. \tag{5}$$

To estimate how many excited states need to be taken into account, we compare the static polarizability calculated from Eq. (4) with the measured atomic polarizability. For Cs the $6P_{1/2}$ and $6P_{3/2}$ states (with $f_{1/2}=0.35$ and $f_{3/2}=0.72$) give a static polarizability of $\alpha_s=5.7\times10^{-23}$ cm^3, while the measured atomic polarizability is $\alpha_s=6.0\times10^{-23}$ cm^3. For Hg the first two excited states ($^1P_1$ with $f=1.2$ and $^3P_1$ with $f=0.025$) contribute about 60% of the static polarizability. All of the frequency shifts considered in this paper depend on the fine or hyperfine interactions in the excited states, which rapidly decrease for higher excited states. Therefore, for a red-detuned trap we only consider the effect of the first two excited states for Cs and Hg. This approximation is accurate to a few percent for Cs and about 30% for Hg. We use the empirical values of the energy levels and the oscillator strengths.

The calculations are performed for a large range of the dipole trap frequency ω. As the frequency is varied, the intensity of the light is adjusted to keep the depth of the trap constant. All Zeeman frequency shifts are proportional to the depth of the trap. We choose a depth of $U=100$ μK. This trap depth has been achieved in a CO_2 laser trap operating at $\lambda=10$ μm [12]. Using sub-Doppler cooling techniques, Cs can be cooled to temperatures on the order of $1-2$ μK [26]; however at such low temperatures spin relaxation rates and frequency shifts due to atomic collisions become very large [2,32]. A temperature on the order of 10 μK may be optimal. The requirement to have a trap with large volume, which can support atoms against gravity, also limits the minimum trap depth. Figure 1 shows the power required to achieve a trap depth of 100 μK with a Gaussian beam focused to a spot size $w_0=100$ μm. The power is plotted vs a scaled frequency (ω/ω_1), where ω_1 is the lowest resonance frequency of the atom ($6P_{1/2}$ state for Cs, 6^3P_1 state for Hg). For very large detuning, $\omega<0.5\omega_1$, a substantial amount of laser power is required. However, this amount of power can be readily obtained from a commercial CO_2 laser.

For small population of the excited states the photon scattering rate is given by the Kramers-Heisenberg formula [27],

$$\gamma_{i\to f}=\frac{\alpha^2\omega^3E_0^2}{3\hbar c}\times\left|\sum_{e,\varepsilon_r}\frac{\langle f|\boldsymbol{\varepsilon}_r^*\cdot\boldsymbol{r}|e\rangle\langle e|\boldsymbol{\varepsilon}\cdot\boldsymbol{r}|i\rangle}{\omega_e-\omega}+\frac{\langle f|\boldsymbol{\varepsilon}^*\cdot\boldsymbol{r}|e\rangle\langle e|\boldsymbol{\varepsilon}_r\cdot\boldsymbol{r}|i\rangle}{\omega_e+\omega}\right|^2, \tag{6}$$

where $\boldsymbol{\varepsilon}_r$ is the polarization of the radiated light. This rate can be divided into the Rayleigh scattering rate $\gamma_h=\gamma_{i\to i}$, which results in heating of the atoms, and the Raman scattering rate $\gamma_R=\Sigma_{i\neq f}\gamma_{i\to f}$, which results in spin relaxation.

We perform all calculations using the formalism of spherical tensors [28,29]. For example,

$$\langle J'IF'm'|\boldsymbol{\varepsilon}\cdot\boldsymbol{r}|JIFm\rangle=\sum_{\rho}(-1)^{\rho}\varepsilon_{\rho}\langle J'IF'm'|r_{-\rho}|JIFm\rangle$$

$$=\sum_{\rho}(-1)^{\rho+F'-m'+J'+I+F+1}\varepsilon_{\rho}\langle J'||r||J\rangle\sqrt{(2F+1)(2F'+1)}$$

$$\times\begin{pmatrix}F' & 1 & F\\ -m' & -\rho & m\end{pmatrix}\begin{Bmatrix}J' & F' & I\\ F & J & 1\end{Bmatrix}. \tag{7}$$

When possible, the reduced radial matrix elements are expressed in terms of the oscillator strengths,

$$|\langle J'||r||J\rangle|^2=\frac{3\hbar(2J+1)}{2m\omega_{JJ'}}f_{J\to J'}. \tag{8}$$

Figure 2 shows the Rayleigh scattering rate for Cs and Hg, while Fig. 3 shows the Raman scattering rate for Cs. For Cs the Raman scattering rate far from the resonance is suppressed compared to the Rayleigh rate by a factor of $(\omega\Delta_{fs}/\omega_1^2)^2$ [10], where $\Delta_{fs}=\omega_{3/2}-\omega_{1/2}$ is the fine-structure splitting of the $6P$ state. Already for $\omega<0.8\omega_1$ the relaxation rate is quite negligible. For Hg the Raman scattering rate is suppressed by $(\omega\Delta_{hfs}/\omega_1^2)^2$, where Δ_{hfs} is the hyperfine splitting of the excited state. The relaxation rate for Hg ranges from 10^{-6} sec^{-1} for $\omega=0.99\omega_1$ to 10^{-20} sec^{-1} for the CO_2 frequency, and is totally negligible.

Thus heating and spin relaxation due to light scattering can be virtually eliminated by using a dipole trap with sufficiently low frequency [10]. In practice, other sources of heating and relaxation have to be considered. The most obvious source of atom loss is due to collision with the background gas. Relaxation and frequency shifts due to cold gas collisions have been considered in [2]. Savard *et al*. [30] have considered the heating of atoms due to vibrations and fluctuations of the laser intensity. Finally, since the atoms sample a distribution of laser intensities in the trap [3], the Zeeman frequency shifts considered below can reduce the transverse spin relaxation time.

III. LIGHT SHIFTS OF THE ZEEMAN LEVELS IN A RED-DETUNED TRAP

The calculations are done using time-dependent perturbation theory. The interaction with the electric field of the trapping beam is given by

$$H=e\boldsymbol{E}\cdot\boldsymbol{r}, \tag{9}$$

with $\boldsymbol{E}$ given by Eq. (3). Throughout the paper e denotes the magnitude of the electron charge. The energy shifts of the Zeeman levels due to interactions with the trapping light can be separated into vector and tensor shifts and expressed in terms of effective operators [13],

$$\Delta E=-\boldsymbol{\mu}\cdot\delta\boldsymbol{B}-\tfrac{1}{6}\boldsymbol{Q}_a:\delta\boldsymbol{\nabla}E, \tag{10}$$

where $\boldsymbol{\mu}$ and $\boldsymbol{Q}_a$ are the atomic magnetic dipole and electric quadrupole operators, while $\delta\boldsymbol{B}$ and $\delta\boldsymbol{\nabla}E$ are the effective magnetic-field and effective electric-field gradient induced by the trapping light.

A. Cesium

1. Vector light shift

The dominant contribution to the vector shift for Cs is given by

$$\Delta E=-\frac{e^2E_0^2}{4\hbar}\sum_{J',F',m'}\left[\frac{\langle J',I,F'm'|\boldsymbol{\varepsilon}\cdot\boldsymbol{r}|J,I,F,m\rangle\langle J,I,F,m|\boldsymbol{\varepsilon}^*\cdot\boldsymbol{r}|J',I,F',m'\rangle}{\omega_{J'}-\omega}\right.$$

$$\left.+\frac{\langle J',I,F'm'|\boldsymbol{\varepsilon}^*\cdot\boldsymbol{r}|J,I,F,m\rangle\langle J,I,F,m|\boldsymbol{\varepsilon}\cdot\boldsymbol{r}|J',I,F',m'\rangle}{\omega_{J'}+\omega}\right], \tag{11}$$

where the sum is taken over the $6P_{1/2}$ and $6P_{3/2}$ states (see discussion after Eq. 5), and $\hbar\omega_{J'}$ is the energy of the excited state relative to the ground state.

The resulting frequency shift can be expressed in terms of the effective magnetic field,

$$\delta\boldsymbol{B}=B_V(|\varepsilon_L|^2-|\varepsilon_R|^2)\hat{\boldsymbol{k}}, \tag{12}$$

where $\hat{\boldsymbol{k}}$ denotes the direction of propagation of the trapping beam. The polarization of the light is expressed in terms of spherical basis vectors, corresponding to the left and right circular polarizations,

$$\boldsymbol{\varepsilon}=\varepsilon_L\frac{-\hat{\boldsymbol{x}}'-i\hat{\boldsymbol{y}}'}{\sqrt{2}}+\varepsilon_R\frac{\hat{\boldsymbol{x}}'-i\hat{\boldsymbol{y}}'}{\sqrt{2}}, \tag{13}$$

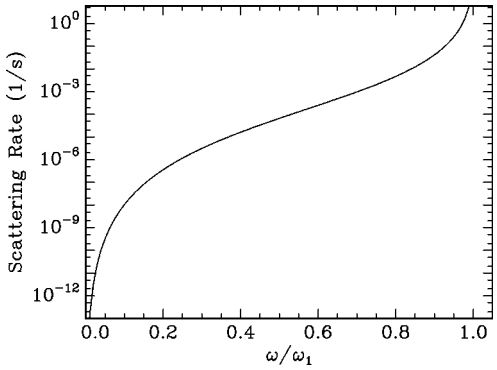

FIG. 3. Raman scattering rate γR for Cs for linearly polarized trapping light.

in the right-handed coordinate system with the z' axis parallel to $\hat{\boldsymbol{k}}$. Thus, the effective magnetic field is proportional to the degree of circular polarization of the trapping light. The frequency shift due to this field is given by

$$\Delta\nu_{F=I\pm1/2}=\pm\frac{g_s\mu_B\delta B}{2I+1}m=\pm\nu_V(|\varepsilon_L|^2-|\varepsilon_R|^2)m\cos\theta, \tag{14}$$

where θ is the angle between $\delta\boldsymbol{B}$ and the static magnetic field $\boldsymbol{B}_S$, which defines the quantization axis. It is assumed that $B_S\gg\delta B$. Depending on the value of B_S, the frequency shift due to the addition of $\delta\boldsymbol{B}$ and $\boldsymbol{B}_S$ in quadrature may also be significant. Figure 4 shows the dependence of ν_V on the frequency of the trapping beam. For low trapping beam frequency the asymptotic form of the shift is approximately given by

$$\nu_V=\frac{2U}{(2I+1)h}\left(\frac{\Delta_{fs}\omega}{\omega_1^2}\right). \tag{15}$$

For the trapping beam frequency near the resonance our results are in agreement with [13].

The vector frequency shift does not depend on the static electric field and, therefore, does not cause a direct systematic error. However, the intensity noise of the trapping laser can limit the achievable sensitivity. In addition, since the atoms sample a distribution of laser intensities, it can result in the reduction of the transverse spin relaxation time.

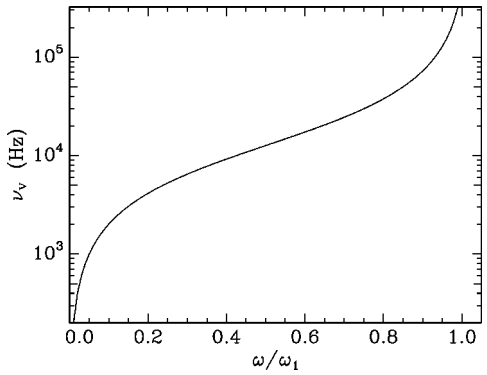

FIG. 4. Vector light shift ν_V in Cs for circularly polarized trapping light.

The vector frequency shift can be substantially reduced by using a linearly polarized trapping beam and by aligning $\delta\boldsymbol{B}$ perpendicular to $\boldsymbol{B}_S$; in other words, directing the trapping beam perpendicular to the static magnetic field. It is reasonable to assume that the helicity of the trapping beam can be reduced to 10^{-4} and the projection of $\delta\boldsymbol{B}$ on $\boldsymbol{B}_S$ to 10^{-3}, reducing the frequency shift by seven orders of magnitude.

Nevertheless, even after such reduction, the vector frequency shift can lead to some problems. For example, for 100-nm detuning to the red of the D_1 line in Cs, the frequency shift is $\Delta\nu=m\times7$ mHz, while for the CO_2 laser ($\lambda=10$ μm), $\Delta\nu=m\times170$ μHz. To avoid the degradation of the short-term sensitivity due to laser intensity fluctuations the intensity noise has to be reduced to less than $0.01\%/\sqrt{\text{Hz}}$ in the first case and less than $0.4\%/\sqrt{\text{Hz}}$ in the second case, assuming that the energy interval between $m=4$ and $m=-4$ states is being measured directly. It is challenging to achieve these requirements. Using a blue-detuned trap, as discussed in Sec. IV, it is possible to reduce the vector light shift by another factor of 100, assuming that the alignment can be controlled at the same level in a more complicated geometry of a blue-detuned trap.

Another possible problem caused by the vector light shift is a reduction of the transverse relaxation time due to an inhomogeneous frequency shift. Assuming that the trap is a harmonic potential near its bottom, the Hamiltonian is given by

$$H=\frac{p^2}{2M}+\frac{1}{2}M\sum_{i=1}^{3}\omega_i^2r_i^2+\frac{g_s\mu_BB_S}{2I+1}F_z, \tag{16}$$

where ω_i are the normal frequencies of the trap. For a Gaussian beam focused to a spot size w_0 and confocal parameter $b=2\pi w_0^2/\lambda$ the normal frequency in the radial direction is $\omega_r^2=4U/w_0^2M$ and in the axial direction is $\omega_a^2=8U/b^2M$, where M is the mass of the atom. Typically, the radial frequency is on the order of 10^4 sec^{-1} and the axial frequency on the order of 10^2 sec^{-1} [30]. Since the frequency shift is proportional to the light intensity it can be represented by a spin-dependent perturbation of the trap frequency,

$$H=\frac{p^2}{2M}+\frac{1}{2}M\sum_i\omega_i^2\left(1+\frac{h\Delta\nu}{U}F_z\right)r_i^2+\frac{g_s\mu_BB_S}{2I+1}F_z. \tag{17}$$

Thus, an atom, which is in an eigenstate of the Hamiltonian (16), is also in an eigenstate of the Hamiltonian (17). The energy of the eigenstates is given by

$$E=\sum_i\hbar\omega_i\left(1+\frac{h\Delta\nu}{2U}F_z\right)(n_i+1/2)+\frac{g_s\mu_BB_S}{2I+1}F_z. \tag{18}$$

Elastic collisions between Cs atoms cause transitions between different levels of the harmonic oscillator potential, which changes the value of the frequency shift. The cross section for Cs-Cs elastic collisions at 10 μK is on the order of $\sigma=10^{-11}$ cm^2, and it rapidly increases for lower temperatures [31]. Assuming atomic density $n=10^{10}$ cm^3 we obtain an elastic collision rate $\gamma_c=n\sigma\bar{v}=0.5$ s^{-1}. Since the collision rate is much smaller than the normal frequencies of the

trap, we are justified in assuming that the atoms are in the eigenstates of the trap Hamiltonian (17) and occasionally make transitions between different eigenstates.

The transverse spin relaxation due to an inhomogeneous frequency shift in the trap is analogous to the problem of spin relaxation due to field inhomogeneities in a gas [32], with γ_c playing the role of the diffusion rate. Since the collision rate γ_c is much smaller than the typical Larmor precession frequency in the field B_S, our conditions are analogous to the high-pressure limit of relaxation in a gas [32]. In this limit only the fluctuations of the longitudinal field cause the relaxation, as was already implicitly assumed in Eq. (17). Thus, the transverse spin relaxation rate is on the order of

$$\frac{1}{T_2}\sim\frac{(\Delta\omega_L)^2}{\gamma_c}, \tag{19}$$

where $\Delta\omega_L$ is a measure of the spread of the Larmor frequencies in the trap. This equation is only valid in the regime of motional narrowing, i.e., for $\Delta\omega_L<\gamma_c$. If $\Delta\omega_L\geqslant\gamma_c$, then $T_2^{-1}\sim\Delta\omega_L$ [32].

If the atoms have a temperature T, then the spread in their energies is on the order of T and the spread in the Larmor frequencies is

$$\Delta\omega_L=\pi\Delta\nu\frac{T}{U}. \tag{20}$$

Thus, for 100-nm red detuning of the trapping beam and $T=10\ \mu$K, $\Delta\omega_L=2\times10^{-2}$ sec^{-1} and the dephasing time between the $m=4$ and $m=-4$ states is $T_2\sim1000$ sec, longer than the expected lifetime of atoms in the trap. However, if the vector frequency shift cannot be reduced by seven orders of magnitude as described above, or if the elastic collision rate is insufficient to satisfy the motional narrowing condition, transverse relaxation due to an inhomogeneous light shift can become a problem.

2. Tensor light shift

To calculate the tensor light shift we take into account the hyperfine structure of the excited states. For large detuning of the trapping beam the hyperfine interaction can be considered as a perturbation,

$$\Delta E=\frac{e^2E_0^2}{4\hbar}\sum_{\substack{J',J''\\F',m'}}\left[\frac{\langle J',I,F'm'|\boldsymbol{\varepsilon}\cdot\mathbf{r}|J,I,F,m\rangle\langle J'',I,F'm'|W|J',I,F'm'\rangle\langle J,I,F,m|\boldsymbol{\varepsilon}^*\cdot\mathbf{r}|J'',I,F',m'\rangle}{(\omega_{J'}-\omega)(\omega_{J''}-\omega)}+\text{c.r.}\right], \tag{21}$$

where c.r. indicates the contribution of the counterrotating component of the electric field. The hyperfine interaction has the following form:

$$W=2\pi a_l\{\boldsymbol{I}\cdot\boldsymbol{I}-[\boldsymbol{s}-3(\boldsymbol{s}\cdot\hat{\boldsymbol{r}})\hat{\boldsymbol{r}}]\cdot\boldsymbol{I}\}+2\pi q\boldsymbol{C}^2{:}\boldsymbol{Q}_n, \tag{22}$$

where $\boldsymbol{C}^2$ and $\boldsymbol{Q}_n$ are the orbital and nuclear quadrupole operators, respectively. We express W in terms of irreducible tensor operators [28],

$$W=2\pi a_l(\boldsymbol{I}\cdot\boldsymbol{I}-\sqrt{10}[\boldsymbol{C}^2\times\boldsymbol{s}]^1\cdot\boldsymbol{I})+2\pi q\boldsymbol{C}^2{:}\boldsymbol{Q}_n. \tag{23}$$

Neglecting the relativistic corrections, the constants a_l and q can be determined from the hyperfine constants A and B of the $P_{3/2}$ state,

$$a_l=A\frac{J(J+1)}{l(l+1)},\quad q=B\frac{2(J+1)}{2J-1}. \tag{24}$$

The hyperfine interaction can couple states of different J and these terms have to be included in Eq. (21). This effect is important when ω is detuned far from the resonance. The matrix element $\langle J'',I,F'm'|W|J',I,F'm'\rangle$ is calculated using the identities for scalar and tensor products of irreducible tensor operators [28].

The resulting frequency shift has the following form:

$$\Delta\nu=\nu_T(F)\,(3\cos^2\phi-1)m^2, \tag{25}$$

where ϕ is the angle between the direction of the electric field of the trapping light (assumed linearly polarized) and the direction of the spin quantization. The contribution of the nuclear quadrupole moment of Cs to the tensor shift is less than 1% and $\nu_T(3)\simeq-\nu_T(4)$. Figure 5 shows the tensor frequency shift for $F=4$.

The tensor light shift approaches a constant at low frequency. It is well known that in the presence of a static electric field the Zeeman levels have a small tensor shift of the form given by Eq. (25) [14,15]. For electric field of 100 kV/cm we obtain $\nu_T=11$ Hz, in agreement with [15]. For $\omega/\omega_1\simeq1$ our results are in agreement with [13].

The problems caused by the tensor light shift are similar to the problems caused by the vector shift, i.e., additional frequency noise due to light-intensity fluctuations and reduction of the transverse relaxation time due to inhomogeneous frequency shifts. To make these problems more manageable, the tensor frequency shift has to be reduced by at least one

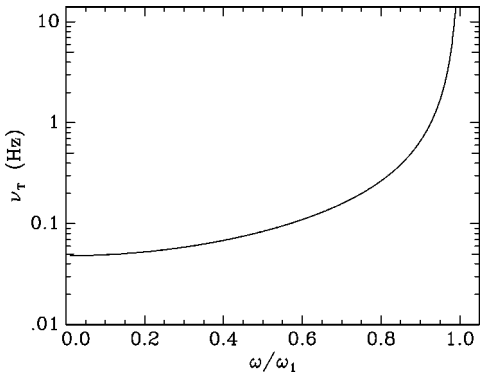

FIG. 5. Tensor light shift $\nu_T(4)$ for Cs for linearly polarized light.

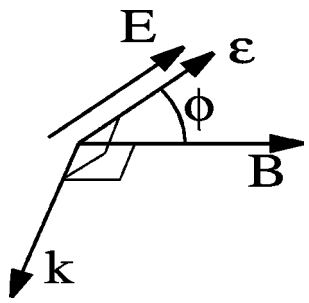

FIG. 6. Relative orientation of the magnetic field $\boldsymbol{B}$, static electric field $\boldsymbol{E}$, the trapping beam wave vector $\boldsymbol{k}$ and the polarization $\boldsymbol{\varepsilon}$ that minimizes the vector and tensor light shifts as well as the tensor shift due to the static electric field, $\phi = 54.7°$.

small factor. This can be accomplished by aligning the electric field of the trapping beam at the magic angle ($\phi = 54.7°$) to the magnetic field, so that $(3\cos^2\phi - 1) = 0$. The configuration of vectors minimizing both vector and tensor light shifts is shown in Fig. 6. Another possibility is to probe the frequency of the transition $m = -4 \rightarrow m = 4$ directly [2,4].

The tensor shift due to the static electric field is proportional to the square of the field and, if the electric field is not perfectly reversed, can result in a false EDM signal. This shift can be reduced in the same way as the tensor light shift. Aligning the static electric field at the magic angle with respect to the magnetic field reduces the sensitivity to an EDM by a factor of 1.7.

B. Mercury

All light shifts in Hg are due to the excited state hyperfine structure. The calculation is complicated by the fact that in Hg two electrons contribute to the hyperfine interaction in the excited state. In addition, because of the breakdown of the *LS* coupling, there is substantial mixing between $^1P_1$ and $^3P_1$ states. The composition of the spectroscopic states in terms of the *LS* states can be determined be diagonalizing the matrix of the electrostatic and spin-orbit interactions [17]. The values of the coupling constants are found from the empirical energies of the $6P$ states. We obtain the following results:

$$^1\overline{P}_1 = 0.979\,^1P_1 + 0.209\,^3P_1, \tag{26}$$

$$^3\overline{P}_1 = 0.979\,^3P_1 - 0.209\,^1P_1, \tag{27}$$

where $^1\overline{P}_1$ and $^3\overline{P}_1$ are the spectroscopic states with energies of 6.704 eV and 4.887 eV and the oscillator strengths of 1.2 and 0.025, respectively.

The hyperfine interaction for Hg is given by

$$W = 2\pi a_l(\boldsymbol{l}_1\cdot\boldsymbol{I} - \sqrt{10}[\boldsymbol{C}_1^2\times\boldsymbol{s}_1]^1\cdot\boldsymbol{I}) + 2\pi q\boldsymbol{C}_1^2:\boldsymbol{Q}_n + 2\pi a_s\boldsymbol{s}_2\cdot\boldsymbol{I}, \tag{28}$$

where the first electron is taken to be in the excited state ($l = 1$) and the second electron in the ground state ($l = 0$). The calculation is simplified by using a $9j$ symbol to recouple the angular momentum,

TABLE I. Hyperfine constants for Hg in GHz; the empirical constants are taken from [34,35].

	$A_{^1\overline{P}_1}$	$B_{^1\overline{P}_1}$	$A_{^3\overline{P}_1}$	$B_{^3\overline{P}_1}$	a_l	a_s
^{199}Hg	−3.57		14.75		1.20	35.16
^{201}Hg	1.32	0.32	−5.45	−0.28	−0.445	12.99
^{201}Hg q		0.85		1.6		

$$|l_1 l_2 L; s_1 s_2 S; J\rangle = \sum_{j_1, j_2} \sqrt{(2L+1)(2S+1)(2j_1+1)(2j_2+1)} \times \begin{Bmatrix} l_1 & l_2 & L \\ s_1 & s_2 & S \\ j_1 & j_2 & J \end{Bmatrix} |l_1 s_1 j_1; l_2 s_2 j_2; J\rangle. \tag{29}$$

The values of a_l, a_s, and q are determined from the empirical hyperfine constants of the spectroscopic states by evaluating $\langle {}^1\overline{P}_1|W|{}^1\overline{P}_1\rangle$ and $\langle {}^3\overline{P}_1|W|{}^3\overline{P}_1\rangle$. The results are given in Table I. We use the value of q determined from $B_{^3\overline{P}_1}$, which is much better known. The calculations can also be performed using jj coupling [33] and taking into account the relativistic corrections. The results of the two methods agree within a few percent for the vector shift and about 30% for the tensor shift.

The vector light shift has the same form as for Cs,

$$\Delta\nu = \nu_V(|\varepsilon_L|^2 - |\varepsilon_R|^2) m\cos\theta, \tag{30}$$

with ν_V for ^{199}Hg shown in Fig. 7. For low trapping beam frequency the asymptotic form is approximately given by

$$\nu_V = \frac{2U}{h}\left(\frac{2\pi a_l \omega}{\omega_1^2}\right). \tag{31}$$

For the CO_2 wavelength ($\lambda = 10\ \mu$m) the shift for ^{199}Hg is $\nu_V = 0.5$ Hz, 2×10^4 times smaller than the shift between $m = 4$ and $m = -4$ states in Cs, while the achievable shot-noise limit is only ten times smaller. Thus the constraints on the alignment, the polarization purity, and the intensity noise of the trapping beam are much less stringent for Hg.

We calculate a typical value of the tensor light shift for ^{201}Hg, which has $I = 3/2$. The shift has the same general form as for Cs,

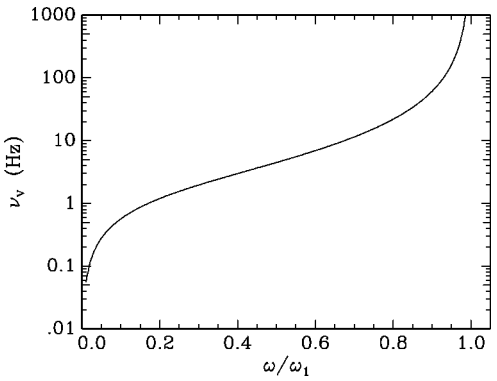

FIG. 7. The vector light shift ν_V for ^{199}Hg for circularly polarized trapping light.

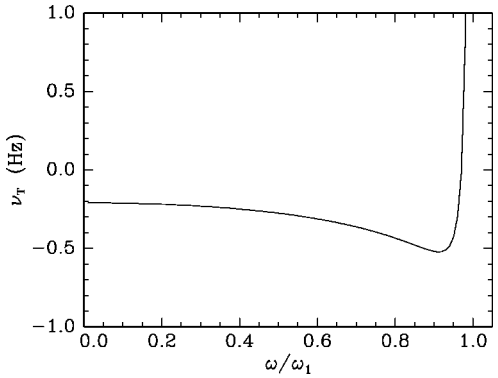

FIG. 8. The tensor light shift ν_T for ^{201}Hg for linearly polarized light.

$$\Delta\nu = \nu_T(3\cos^2\phi - 1)m^2, \tag{32}$$

with ν_T shown in Fig. 8. For large detuning the tensor shift due to the $^1\overline{P}_1$ state dominates, but the contribution of the $^3\overline{P}_1$ state, which has the opposite sign, becomes large near the resonance. The tensor light shift for ^{201}Hg is comparable to the shift for Cs, while the shot-noise limit is ten times smaller and the required frequency sensitivity is nearly three orders of magnitude smaller. Fortunately, for ^{199}Hg, ^{171}Yb, and other elements with nuclear spin $I=1/2$, the tensor shifts (both ac and dc) are totally absent. However, for heavy radioactive elements (Ra, Rn), which do not have a convenient spin 1/2 isotope, the tensor shifts may present a very serious problem.

IV. CESIUM LIGHT SHIFTS IN A BLUE-DETUNED TRAP

In this section we calculate vector and tensor frequency shifts for a blue-detuned optical trap. In such a trap the atoms are repelled from the regions of high laser intensity and thus experience a smaller average frequency shift. For Cs atoms such a trap can be realized, for example, with an Ar^+ laser [3,36,37]. In Fig. 9 we plot the power necessary to achieve 100-μK wall height with a Gaussian light sheet focused to 10×100-μm beam waist. For diamagnetic atoms, like Yb and Hg, blue detuned traps are more difficult to realize due to the lack of powerful cw lasers in deep UV. A blue-detuned trap for Yb could possibly be constructed using UV lines from an Ar^+ laser.

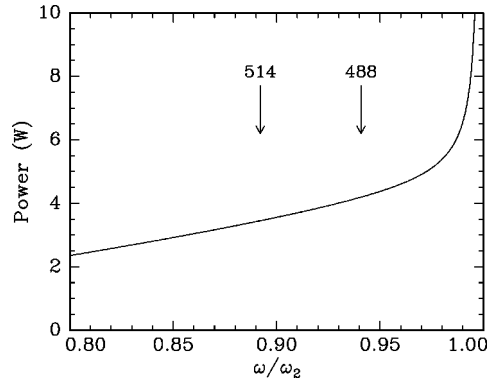

FIG. 9. The power required in a blue-detuned trap to achieve 100-μK wall height with a cylindrical Gaussian beam focused to 10×100-μm waist. ω_2 is the frequency of the $6S_{1/2}$-$7P_{1/2}$ transition. Arrows indicate the two dominant lines of an Ar^+ laser.

The average Zeeman frequency shift experienced by an atom in a blue-detuned trap depends critically on the trap geometry. Several different geometries have been realized [3,36,37] so far. Here we make a rough estimate of the average frequency shift in an open top square box trap made with five perpendicular sheets of light.

The Zeeman frequency shift is proportional to the average value of the trapping potential experienced by the atom in the trap. First, consider an atom with mass M, initial velocity v_i, and kinetic energy $U_i = Mv_i^2/2$ impinging on a Gaussian wall of light with beam waist w. The potential of the wall is given by

$$U(x) = U_0 e^{-x^2/8w^2}. \tag{33}$$

The total phase shift experienced by the atom during collision with the wall is

$$\Delta\phi = \frac{2}{\hbar}\int_{\infty}^{x_t} \frac{U(x)dx}{\sqrt{\frac{2}{M}[U_i - U(x)]}} = U_i t_{ph}/\hbar. \tag{34}$$

Here x_t is the classical turning point given by $U(x_t) = U_i$, and the last equality is used to define the equivalent dephasing time t_{ph}. We calculated the ratio of the dephasing time t_{ph} to the wall traversing time $t_{tr} = w/v_i$ and found that it depends only weakly on the ratio U_0/U_i. We obtain $t_{ph}/t_{tr} \sim 0.4$ for $U_0/U_i > 5$.

Thus, for an atom at temperature T confined in the horizontal direction by two pairs of walls separated by distance d each, the average trapping potential energy due to thermal motion is approximately given by

$$\langle U\rangle_{th} \sim 0.4\frac{w}{d}kT. \tag{35}$$

Using similar considerations, one can show that for an atom held against gravity on a sheet of light with focal waist w the average trapping potential energy due to gravity is approximately given by

$$\langle U\rangle_g \sim 0.08\,Mgw, \tag{36}$$

and is relatively insensitive to U_0 and kT. The energy due to thermal motion in the vertical direction is smaller then $\langle U\rangle_g$ for a large range of parameters. An optimal trap configuration minimizing the average light shift is a large box made with tightly focused walls of light, so that $d \gg w$ and $Mgw \ll kT$. The blue-detuned traps realized so far have $d \sim w$ and $Mgw \sim kT$ [3,36] or $d \ll w$ and $Mgw \gg kT$ [37].

Thus, in blue-detuned traps the average trapping potential energy experienced by the atoms can be less than thermal energy kT. In red-detuned traps the average trapping potential energy is equal to the trap depth. A trap depth on the order of 10 kT is required to prevent loss of atoms due to evaporation. In the following calculations we assume that the average trapping potential energy experienced by the atoms is 1 μK, which is also similar to the average energy measured in a blue-detuned trap by Davidson *et al.* [3].

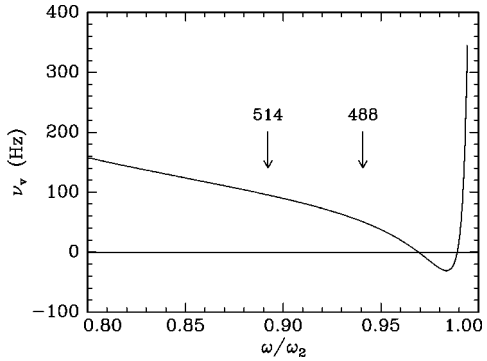

FIG. 10. The vector light shift experienced by Cs atoms in a blue detuned trap with an average trapping potential energy of 1 μK. Arrows indicate the two dominant lines of an Ar^+ laser.

For calculation of the frequency shifts in a blue-detuned trap made using Ar^+ lines it is necessary to include the contribution of the second resonance line of Cs. In fact, its contribution actually reduces the frequency shifts. The Rayleigh scattering rate in such a blue-detuned trap is about 0.01 sec^{-1} and the Raman scattering rate is 5×10^{-6} sec^{-1}. The vector light shift is shown in Fig. 10. The frequency shift is plotted as a function of the ratio ω/ω_2, where ω_2 is the resonance frequency of the $6S_{1/2}$-$7P_{1/2}$ transition at 459.3 nm. Due to the contribution of the second resonance line the vector frequency shift vanishes at 474 nm and 464 nm, and is suppressed for 488-nm Ar^+ line. In Fig. 11 we show the average tensor frequency shift experienced by Cs atoms in the blue-detuned trap. The frequency shift is also suppressed due to the contribution of the second resonance line.

Thus, the Cs vector and tensor frequency shifts in a blue-detuned trap formed with the 488-nm Ar^+ line are approximately 100 times smaller than the shifts in a very far red-detuned laser trap. If the beam alignment can be equally well controlled in a more complicated geometry of a blue-detuned trap, it can give much smaller Zeeman light shifts for Cs atoms.

V. FREQUENCY SHIFTS DUE TO PARITY MIXING BY THE STATIC ELECTRIC FIELD

In the presence of a static electric field the atomic levels acquire a small admixture of opposite parity states. This allows an interference of the electric dipole amplitude driven by the optical field with higher-order amplitudes which are normally forbidden by parity selection rules. The modification of the light absorption cross section due to this effect was considered for Rb [16] and for Hg [17]. The effect has been observed experimentally in Rb [38]. Here we consider the Zeeman frequency shifts due to magnetic dipole and electric quadrupole amplitudes driven by the optical field. The calculations are only performed for the red-detuned optical trap. The calculations for blue-detuned trap are much more complicated because many additional excited states must be taken into account.

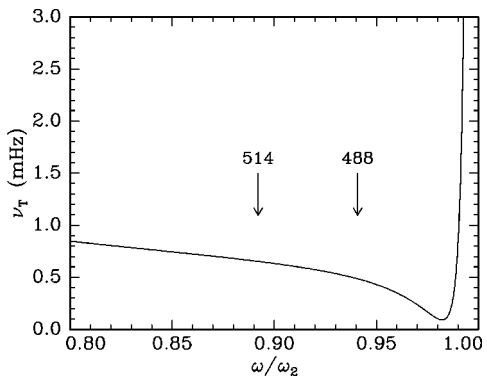

FIG. 11. The tensor light shift experienced by Cs atoms in a blue-detuned trap with an average trapping potential energy of 1 μK. Arrows indicate the two dominant lines of an Ar^+ laser.

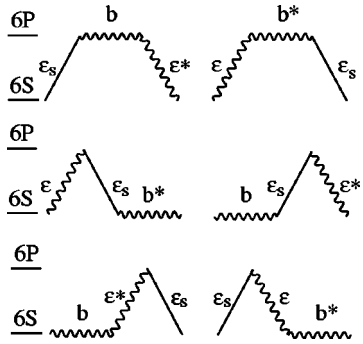

FIG. 12. All possible permutations of the matrix elements which contribute to Eq. (38). ε and b denote electric- and magnetic dipole transitions induced by the trapping beam, ε_s denotes mixing by the static electric field.

We start with the calculation of the shift due to magnetic dipole transitions in Cs. The magnetic dipole interaction of the valence electron with the magnetic field of the light wave has the following form:

$$H=-\boldsymbol{M}\cdot\boldsymbol{B}=\frac{E_0\mu_B}{2}(\boldsymbol{L}+2\boldsymbol{S})\cdot(\hat{\boldsymbol{b}}\,e^{-i\omega t}+\hat{\boldsymbol{b}}^*\,e^{i\omega t}), \quad (37)$$

where $\hat{\boldsymbol{b}}$ denotes the direction of the magnetic field in the optical wave, $\hat{\boldsymbol{b}}=\hat{\boldsymbol{k}}\times\hat{\boldsymbol{\varepsilon}}$. The energy shift is given by

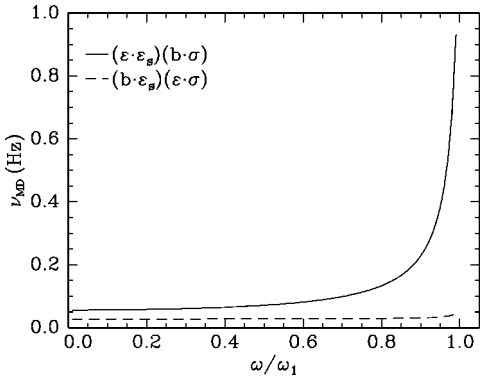

FIG. 13. Zeeman frequency shift for Cs due to magnetic dipole transitions, ν^1_{MD} (solid line) and ν^2_{MD} (broken line).

$$\Delta E=\frac{e^2\mu_B E_0^2 E_S}{4\hbar^2}\sum_{J',J'',m',m''}\left[\frac{\langle J',m'|\boldsymbol{\varepsilon}\cdot\boldsymbol{r}|J,m\rangle\langle J'',m''|\boldsymbol{b}^*\cdot(\boldsymbol{L}+2\boldsymbol{S})|J',m'\rangle\langle J,m|\boldsymbol{\varepsilon}_s\cdot\boldsymbol{r}|J'',m''\rangle}{(\omega_{J'}-\omega)(\omega_{J''}-\omega)}\right.$$
$$\left.+\frac{\langle J,m'|\boldsymbol{b}\cdot(\boldsymbol{L}+2\boldsymbol{S})|J,m\rangle\langle J',m'|\boldsymbol{\varepsilon}^*\cdot\boldsymbol{r}|J,m'\rangle\langle J,m|\boldsymbol{\varepsilon}_s\cdot\boldsymbol{r}|J',m'\rangle}{\omega_{J'}(\omega_{J'}-\omega)}+\text{perm.}+\text{c.r.}\right] \tag{38}$$

where $\boldsymbol{\varepsilon}_s$ denotes the direction of the static electric field $\boldsymbol{E}_S=E_S\hat{\boldsymbol{\varepsilon}}_s$. There are six possible permutations of the matrix elements (denoted perm.) shown graphically in Fig. 12 plus the counter-rotating terms (obtained by taking the complex conjugate of the matrix element and replacing $\omega\rightarrow-\omega$). The sum over J' and J'' is taken over the $6P_{1/2}$ and $6P_{3/2}$ states.

The frequency shift depends on four vectors, $\hat{\boldsymbol{\varepsilon}}$, $\hat{\boldsymbol{\varepsilon}}_s$, $\hat{\boldsymbol{b}}$, and $\hat{\boldsymbol{\sigma}}$, where $\hat{\boldsymbol{\sigma}}$ is the direction of the spin quantization. A product of all four vectors is P and T symmetric. Only two nonzero vector products can be formed,

$$(\hat{\boldsymbol{b}}\cdot\hat{\boldsymbol{\sigma}})(\hat{\boldsymbol{\varepsilon}}\cdot\hat{\boldsymbol{\varepsilon}}_s)\quad\text{and}\quad(\hat{\boldsymbol{b}}\cdot\hat{\boldsymbol{\varepsilon}}_s)(\hat{\boldsymbol{\varepsilon}}\cdot\hat{\boldsymbol{\sigma}}). \tag{39}$$

We parametrize the frequency shift due to magnetic dipole transitions as follows:

$$\Delta\nu_{F=I\pm1/2}=\mp[\nu_{MD}^1(\hat{\boldsymbol{b}}\cdot\hat{\boldsymbol{\sigma}})(\hat{\boldsymbol{\varepsilon}}\cdot\hat{\boldsymbol{\varepsilon}}_s)+\nu_{MD}^2(\hat{\boldsymbol{b}}\cdot\hat{\boldsymbol{\varepsilon}}_s)(\hat{\boldsymbol{\varepsilon}}\cdot\hat{\boldsymbol{\sigma}})]m, \tag{40}$$

with the results for ν_{MD} shown in Fig. 13. All numerical calculations are done for $E_s=100$ kV/cm.

For low trapping beam frequency the shift approaches a constant value that is approximately given by

$$\Delta\nu_{F=I\pm1/2}=\mp\frac{4U}{h(2I+1)}\frac{\Delta_{fs}\mu_B E_s}{(\hbar\omega_1)^2}\times[(\hat{\boldsymbol{b}}\cdot\hat{\boldsymbol{\sigma}})(\hat{\boldsymbol{\varepsilon}}\cdot\hat{\boldsymbol{\varepsilon}}_s)+(\hat{\boldsymbol{b}}\cdot\hat{\boldsymbol{\varepsilon}}_s)(\hat{\boldsymbol{\varepsilon}}\cdot\hat{\boldsymbol{\sigma}})/2]m. \tag{41}$$

The shift is proportional to the fine structure Δ_{fs} of the $6P$ state.

The electric quadrupole interaction is given by

$$H=\frac{e}{6}\sum_{ij}(3r_ir_j-\delta_{ij}r^2)\frac{\partial E_i}{\partial r_j}=\frac{e}{2}\sum_q(-1)^m Q_{2m}T_{2-m}, \tag{42}$$

where Q_{2m} is the orbital quadrupole spherical tensor and T_{2m} is the quadrupole spherical tensor of the electric-field gradient. The electric-field gradient tensor of the trapping beam is given by

$$\frac{\partial E_i}{\partial r_j}=\frac{E_0}{2}[i\varepsilon_i k_j e^{i(k\cdot r-\omega t)}-i\varepsilon_i^* k_j e^{-i(k\cdot r-\omega t)}]. \tag{43}$$

The spherical quadrupole components are formed from the Cartesian components in accordance with the prescription given in [29]. The frequency shift comes from the contribution of the $6P$ and $6D$ states. The sum over J quantum numbers is suppressed in Eq. (44). Possible permutations of the matrix elements are shown graphically in Fig. 14.

$$\Delta E=\frac{e^3E_0E_s}{4\hbar^2}\sum\left[\frac{\langle P|\boldsymbol{\varepsilon}\cdot\boldsymbol{r}|S\rangle\langle P|\boldsymbol{Q}^*:\boldsymbol{T}|P\rangle\langle S|\boldsymbol{\varepsilon}_s\cdot\boldsymbol{r}|P\rangle}{(\omega_P-\omega)(\omega_P-\omega)}\right.$$
$$\left.+\frac{\langle D|\boldsymbol{Q}:\boldsymbol{T}|S\rangle\langle P|\boldsymbol{\varepsilon}^*\cdot\boldsymbol{r}|D\rangle\langle S|\boldsymbol{\varepsilon}_s\cdot\boldsymbol{r}|P\rangle}{(\omega_D-\omega)(\omega_P-\omega)}+\text{perm.}+\text{c.r.}\right]. \tag{44}$$

The frequency shift due to the electric quadrupole transitions depends on four vectors $\hat{\boldsymbol{\varepsilon}}$, $\hat{\boldsymbol{\varepsilon}}_s$, $\hat{\boldsymbol{k}}$, and $\hat{\boldsymbol{\sigma}}$; and $\hat{\boldsymbol{\varepsilon}}$ appears twice. One can form three nonzero vector products,

$$[(\hat{\boldsymbol{\sigma}}\times\hat{\boldsymbol{k}})\cdot\hat{\boldsymbol{\varepsilon}}](\hat{\boldsymbol{\varepsilon}}\cdot\hat{\boldsymbol{\varepsilon}}_s),\ [(\hat{\boldsymbol{\varepsilon}}_s\times\hat{\boldsymbol{k}})\cdot\hat{\boldsymbol{\varepsilon}}](\hat{\boldsymbol{\varepsilon}}\cdot\hat{\boldsymbol{\sigma}}),\ \text{and}\ [(\hat{\boldsymbol{\sigma}}\times\hat{\boldsymbol{k}})\cdot\hat{\boldsymbol{\varepsilon}}_s](\hat{\boldsymbol{\varepsilon}}\cdot\hat{\boldsymbol{\varepsilon}}). \tag{45}$$

However, the first two products are equal to the products given in Eq. (39), while the last product can be reduced to a linear combination of the first two. Thus, the vector dependence of the electric quadrupole and magnetic dipole contributions is identical. The shift can be parametrized in the same form,

$$\Delta\nu_{F=I\pm1/2}=\pm[\nu_{EQ}^1(\hat{\boldsymbol{b}}\cdot\hat{\boldsymbol{\sigma}})(\hat{\boldsymbol{\varepsilon}}\cdot\hat{\boldsymbol{\varepsilon}}_s)+\nu_{EQ}^2(\hat{\boldsymbol{b}}\cdot\hat{\boldsymbol{\varepsilon}}_s)(\hat{\boldsymbol{\varepsilon}}\cdot\hat{\boldsymbol{\sigma}})]m. \tag{46}$$

Our results for ν_{EQ} are shown in Fig. 15. Bates-Damgaard approximation was used to evaluate the radial matrix ele-

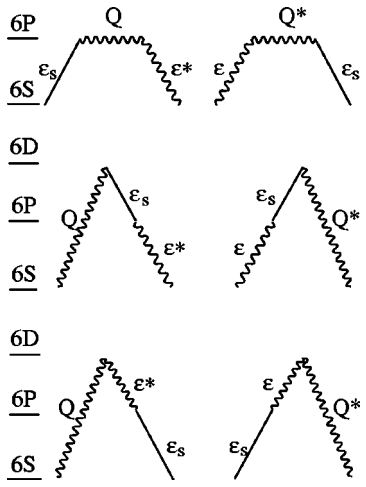

FIG. 14. All possible permutations of the matrix elements, which contribute to Eq. (44). ε denotes the electric dipole transitions and Q denotes the electric quadrupole transitions induced by the trapping beam; ε_s denoted mixing by the static electric field.

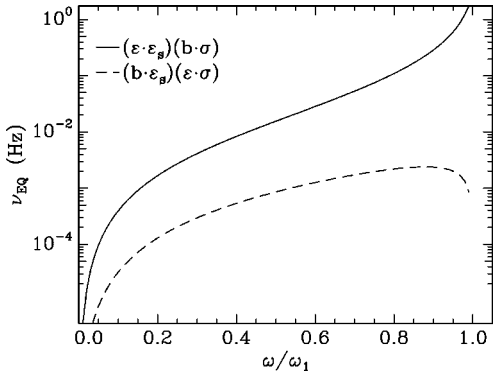

FIG. 15. Shifts of the Zeeman levels due to the electric quadrupole transitions in Cs, ν^1_{EQ} (solid line) and ν^2_{EQ} (broken line).

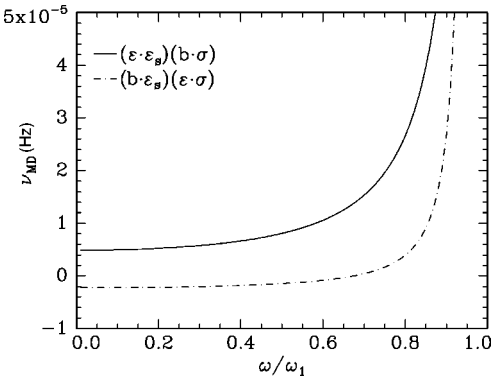

FIG. 17. Frequency shift due to magnetic dipole transitions in Hg, ν^1_{MD} (solid line) and ν^2_{MD} (broken line).

ments in this case. Note that the shift due to the electric quadrupole transitions has an opposite sign compared to the shift due to the magnetic dipole transitions. The two shifts are comparable in size near the resonance, but the quadrupole shift drops as ω due to the factor of k in Eq. (43). The vector product $(\hat{\boldsymbol{b}}\cdot\hat{\boldsymbol{\sigma}})(\hat{\boldsymbol{\varepsilon}}\cdot\hat{\boldsymbol{\varepsilon}}_s)$ gives the dominant contribution near the resonance for both magnetic dipole and electric quadrupole transitions, in agreement with the results in [16].

To minimize the magnetic dipole and the electric quadrupole shifts one can orient the trapping beam direction and polarization as shown in Fig. 16. This orientation suppresses both vector products in Eq. (39) by one small factor and also suppresses the vector light shift, Eq. (14), by two small factors. However, the tensor light shift, Eq. (25), is not suppressed. Assuming a factor of 10^3 suppression of the shift due to the magnetic dipole transitions, Eq. (40), it would still be on the order of $m\times 50$ μHz for trapping frequency $\omega < 0.5\omega_1$, much larger than the required accuracy. The shift can be further reduced by frequently reversing the direction $\hat{\boldsymbol{k}}$ or using a standing wave. However, if the tensor light shift presents a more serious problem, one would align the electric field of the light and the static electric field at the magic angle, as shown in Fig. 6. In this case the first term in Eq. (39) is not suppressed, but the second is suppressed. One can then use a standing wave to suppress the parity mixing shifts, although the intensity of the two counterpropagating beams would have to be balanced to 1×10^{-7} for the systematic error due to this shift to be comparable to the final statistical error of 50 nHz.

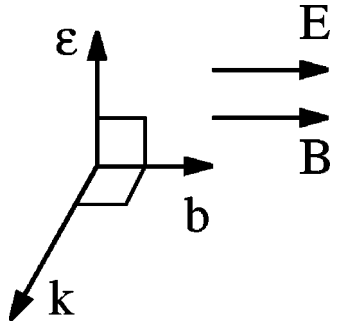

FIG. 16. Relative orientation of the magnetic field $\boldsymbol{B}$, static electric field $\boldsymbol{E}$, the trapping beam wave vector $\boldsymbol{k}$ and the polarization $\boldsymbol{\varepsilon}$ that minimizes the shifts due to parity mixing induced by the electric field as well as the vector light shift.

Finally, we calculate the frequency shift due to magnetic dipole transitions in Hg. The shift is nonzero only if the hyperfine interactions in the exited state are taken into account. Since both W and M operators can change the J quantum number, the metastable $^3P_0$ and $^3P_2$ states also contribute to the shift. The shift has the same vector form as for Cs,

$$\Delta\nu=[\,\nu^1_{MD}(\hat{\boldsymbol{b}}\cdot\hat{\boldsymbol{\sigma}})(\hat{\boldsymbol{\varepsilon}}\cdot\hat{\boldsymbol{\varepsilon}}_s)+\nu^2_{MD}(\hat{\boldsymbol{b}}\cdot\hat{\boldsymbol{\varepsilon}}_s)(\hat{\boldsymbol{\varepsilon}}\cdot\hat{\boldsymbol{\sigma}})\,]m, \quad (47)$$

with ν_{MD} shown in Fig. 17. The size of the shift is five orders of magnitude smaller than for Cs. Since the tensor shift does not exist for nuclei with $I=1/2$, the magnetic dipole shift can be suppressed by one small factor, as shown in Fig. 16, so it becomes comparable to the statistical uncertainty. Further suppression can be easily achieved by periodically reversing the direction of $\hat{\boldsymbol{k}}$.

VI. CONCLUSIONS

In this paper we have calculated the Zeeman frequency shifts experienced by atoms trapped in an optical dipole trap. These shifts are particularly important for applications of such a trap to searches for EDM. The shifts can be divided into three classes: vector light shifts, tensor light shifts, and shifts due to parity mixing induced by a static electric field. The typical size of all shifts considered here is much larger than the sensitivity required for EDM measurements. The frequency shifts for Cs in a red-detuned trap are four to five orders of magnitude larger than for Hg. However, for Cs atoms the shifts can be reduced by a factor of 100 using a blue-detuned trap. By a careful choice of the orientation of the relevant vectors it appears that all frequency shifts may be suppressed to manageable levels.

The vector light shift due to circular polarization of the trapping light is by far the largest. It can be reduced by using linearly polarized trapping light directed perpendicular to the applied magnetic field.

The tensor shifts are produced by the trapping beam and the static electric field. They are absent for ^{199}Hg and other

nuclei with $I = 1/2$. It is possible to suppress these effects by aligning the electric fields at the magic angle to the quantization axis.

The shifts due to parity mixing by the electric field are proportional to the electric field and thus mimic an EDM. These shifts can be suppressed by a certain orientation of the relevant vectors or by using a standing wave for the trapping beam.

ACKNOWLEDGMENT

This work was supported by the National Science Foundation under Grant No. PHY-9732513.

[1] S.M. Barr, Int. J. Mod. Phys. A **8**, 209 (1993).
[2] M. Bijlsma, B.J. Verhaar, and D.J. Heinzen, Phys. Rev. A **49**, R4285 (1994).
[3] N. Davidson, H.J. Lee, C.S. Adams, M. Kasevich, and S. Chu, Phys. Rev. Lett. **74**, 1311 (1995).
[4] E.D. Commins, S.B. Ross, D. DeMille, and B.C. Regan, Phys. Rev. A **50**, 2960 (1994).
[5] J.P. Jacobs, W.M. Klipstein, S.K. Lamoreaux, B.R. Heckel, and E.N. Fortson, Phys. Rev. A **52**, 3521 (1995).
[6] S.A. Murthy, D. Krause, Z.L. Li, and L.R. Hunter, Phys. Rev. Lett. **63**, 965 (1989).
[7] K.F. Smith *et al.*, Phys. Lett. B **234**, 191 (1990).
[8] I.S. Altarev *et al.*, Phys. Lett. B **276**, 242 (1992).
[9] J.D. Miller, R.A. Cline, and D.J. Heinzen, Phys. Rev. A **47**, R4567 (1993).
[10] T. Takekoshi, J.R. Yeh, and R.J. Knize, Opt. Commun. **114**, 421 (1995).
[11] R.A. Cline, J.D. Miller, M.R. Matthews, and D.J. Heinzen, Opt. Lett. **19**, 207 (1994).
[12] T. Takekoshi and R.J. Knize, Opt. Lett. **21**, 77 (1996).
[13] W. Happer and B.S. Marthur, Phys. Rev. **163**, 12 (1967); **171**, 11 (1968).
[14] P.G.H. Sandars, Proc. Phys. Soc. London **92**, 857 (1967).
[15] H. Gould, E. Lipworth, and M.C Weisskopf, Phys. Rev. **188**, 24 (1969).
[16] J. Hodgdon, B.R. Heckel, and E.N. Fortson, Phys. Rev. A **43**, 3343 (1991).
[17] S.K. Lamoreaux and E.N. Fortson, Phys. Rev. A **46**, 7053 (1992).
[18] G.D. Sprouse, L.A. Orozco, J.E. Simsarian, and W.Z. Zhao, Nucl. Phys. A **630**, 316 (1998).
[19] P.G.H. Sandars, Phys. Rev. Lett. **14**, 194 (1965); **22**, 290 (1966).
[20] B. P. Das (private communication).
[21] Y. Takahashi, M. Fujimoto, T. Yabuzaki, A.D. Singh, M.K. Samal, and B.P. Das, in *Proceedings of CP Violation and its Origins*, edited by K. Hagiwara (KEK Reports, Tsukuba, 1997).
[22] V. Spevak, N. Auerbach, and V.V. Flambaum, Phys. Rev. C **56**, 1357 (1997).
[23] D. Weiss (private communication).
[24] D.M. Stamper-Kurn, M.R. Andrews, A.P. Chikkatur, S. Inouye, H.-J. Miesner, J. Stenger, and W. Ketterle, Phys. Rev. Lett. **80**, 2027 (1998).
[25] K.D. Bonin and M.A. Kadar-Kallen, Phys. Rev. A **47**, 944 (1993).
[26] K. Gibble, S. Chang, and R. Legere, Phys. Rev. Lett. **75**, 2666 (1995).
[27] R. London, *The Quantum Theory of Light* (Clarendon, Oxford, 1983).
[28] I.I. Sobelman, *Atomic Spectra and Radiative Transitions* (Springer, Berlin, 1996).
[29] D.A. Varshalovich, A.N. Moskalev, and V.K. Khersonskii, *Qunatum Theory of Angular Momentum* (World Scientific, Singapore, 1988).
[30] T.A. Savard, K.M. O'Hara, and J.E. Thomas, Phys. Rev. A **56**, R1095 (1997).
[31] M. Arndt, M. Ben Daham, D. Guery-Odelin, M.W. Reynolds, and J. Dalibard, Phys. Rev. Lett. **79**, 625 (1997).
[32] G.D. Cates, S.R. Schaefer, and W. Happer, Phys. Rev. A **37**, 2877 (1988).
[33] W.G. Schweitzer, J. Opt. Soc. Am. **53**, 1055 (1963).
[34] A. Corney, *Atomic and Laser Spectroscopy* (Oxford University Press, Oxford, 1977).
[35] C. Bousquet, E. Leboucher, and N. Bras, Nouv. Res. Opt. **5**, 121 (1974).
[36] T. Kuga, Y. Torii, N. Shiokawa, T. Hirano, Y. Shimizu, and H. Sasada, Phys. Rev. Lett. **78**, 4713 (1997).
[37] Yu.B. Ovchinnikov, I. Manek, A.I. Sidorov, G. Wasik, and R. Grimm, Europhys. Lett. **43**, 510 (1998).
[38] Xu Chen, F.R. Huang-Hellinger, B.R. Heckel, and E.N. Fortson, Phys. Rev. A **50**, 4729 (1994).